Available online at www.sciencedirect.com
SCIENCE DIRECT
Biochemical and Biophysical Research Communications 347 (2006) 83–88
BBRC
www.elsevier.com/locate/ybbrc

Real-time chemiluminescent imaging and detection of reactive oxygen species generated in the UVB-exposed human skin equivalent model ☆

Hiroyuki Yasui [a], Tomohiro Hakozaki [b], Akira Date [b], Takashi Yoshii [b], Hiromu Sakurai [a,*]

[a] *Department of Analytical and Bioinorganic Chemistry, Kyoto Pharmaceutical University, 5 Nakauchi-cho, Misasagi, Yamashina-ku, Kyoto 607-8414, Japan*
[b] *Kobe Technical Center, Procter & Gamble Far East, Inc., Kobe 658-0032, Japan*

Received 17 May 2006
Available online 16 June 2006

Abstract

The objective of this study is to image and detect reactive oxygen species (ROS) generated in the UVB-exposed three-dimensional human skin equivalent model (HSEM), EpiDerm™ 200, because the alternative system needs to be urgently established as a replacement for the skin of experimental animals. Evidence that the ROS generation is enhanced in the skin of live animals after the UVB exposure was already obtained, by using the real-time chemiluminescent (RT-CL) method consisting of a sensitive CL probe (CLA) and an ultra-low light imaging apparatus. In this study, CL emission due to the reaction of CLA with endogenously generated ROS increased significantly in the UVB-treated HSEM compared with that in the intact HSEM, the maximum level being observed at a dose of 27 mJ/cm^2. ROS under UVB exposure was identified to be $\cdot O_2^-$ and $^1O_2$ as observed by suppressive effects of SOD and β-carotene topically applied on sample surface before the UVB exposure. The results for UVB-induced ROS generation in HSEM were consistent with those observed in the skin of live animals. HSEM combined with the RT-CL method was shown to be useful system not only to predict UVB-induced ROS-related skin responses in human but also to find protective agents against UVB-stimulated oxidative stress in place of animals and *ex vivo* human skin.

Keywords: Chemiluminescent detection; Ultra-low light imaging; UVB exposure; Reactive oxygen species (ROS); Superoxide anion radical ($\cdot O_2^-$); Singlet oxygen ($^1O_2$); Human skin equivalent model (HSEM); EpiDerm™ 200; Radical scavengers

Oxidative cellular stress and DNA damage caused by ultraviolet (UV) radiation have been recognized to participate in pathogenesis of the skin [1]. Among several oxidative stressors, reactive oxygen species (ROS) has been suggested to relate to the process of UV radiation-induced skin damage including premature skin aging (photo-aging), immunomodulation, and skin cancer [2,3]. It has already been shown that ROS level increased in the skin of animals after UV exposure [4–6] and then the cell injury such as apoptosis and skin cancer was found in the epidermis by ROS [7]. Antioxidative enzymes such as superoxide dismutase (SOD), catalase (CAT), and glutathione peroxidase (GSH-Px) play important roles on protecting the skin against degenerative changes [8,9]. To examine the relationship between the oxidative stress due to ROS produced by UV exposure and several skin pathogeneses, it is essential to observe the *in vivo* and real-time changes in the skin. However, because ROS is extremely short-lived and essentially non-emissive, ROS is difficult to detect directly. For this purpose, several evaluation methods such as chemiluminescence [10], photoemission [11], and fluorescence [12] as well as ESR spectroscopy using spin probes [13] have been used. In 2000, we developed a unique technique based on an *in vivo* real-time chemiluminescent (RT-CL) detection and two-dimensional ultra low-light imaging of

☆ *Abbreviations:* CL, chemiluminescence; CLA (*cypridina hilgendorfii* luciferin analog), 2-methyl-6-phenyl-3,7-dihydroimidazo-[1,2-*a*]-pyrazin-3-one; ROS, reactive oxygen species; $\cdot O_2^-$, superoxide anion radical; $^1O_2$, singlet oxygen, H_2O_2, hydrogen peroxide; $\cdot OH$, hydroxyl radical; UVB, ultraviolet light B; SOD, superoxide dismutase; BCR, β-carotene; HSEM, human skin equivalent model; AUC, area under the curve for time-dependent chemiluminescent profile; CCD, charge-coupled device.

* Corresponding author. Fax: +81 75 595 4753.
E-mail address: sakurai@mb.kyoto-phu.ac.jp (H. Sakurai).

0006-291X/$ - see front matter © 2006 Elsevier Inc. All rights reserved.
doi:10.1016/j.bbrc.2006.06.046

endogenously generated ROS in the skin of living animals after UVA light irradiation [4], using a sensitive CL probe, CLA, which was shown to react with $^{\cdot}O_2^-$ and $^1O_2$ [14]. This method has been successfully used for finding protective agents or materials against UV light-induced skin damage as well as for characterizing the ROS generated in the UV (UVA and UVB) light-exposed animal skin [5,15].

Since 1981, several types of reconstructed human skin equivalent models (HSEM) have been developed. These models have been used to reproduce many morphological characteristics of human skin [16], and provided as the means for studying pathophysiology such as photo-aging in the skin [17]. Such HSEM enabled us to examine the skin irritation and safety assessments for chemicals and product formulations as a pre-clinical screening system, and to facilitate the design of safe and efficient human studies. *In vitro* responses in the HSEM were compared directly to *in vivo* human skin responses, in which representative chemicals and products were applied on the stratum corneum surface of the skin models [18,19]. Thus, the potential of HSEM has been established as an *in vitro* pre-clinical screening system for examining *in vivo* human skin irritation responses [20]. Three-dimensional HSEMs, EpiDerm™ 200 (epidermis) and Epiderm-FT™ 200 (epidermis/dermis), have been developed in place of experimental animals and *ex vivo* human skin in 2002 [21], and applied to several trials [22]. However, to the best of our knowledge, there are few reports for detecting ROS generation in the HSEMs, in which two-photon fluorescence imaging is used only to observe ROS induction after a relatively low dose (20 mJ/cm^2) of UVB exposure [23]. Then, we applied our sensitive real-time chemiluminescent method for detection of ROS generation in the HSEM, EpiDerm™ 200, under UVB light exposure to examine the usefulness of this model and its replacement for animals in terms of UVB-induced ROS generation and its related biological response.

Materials and methods

Materials. CLA, 2-methyl-6-phenyl-3,7-dihydroimidazo-[1,2-*a*]-pyrazin-3-one, and β-carotene (BCR) were purchased from Tokyo Kasei Organic Chemicals (Tokyo, Japan). Superoxide dismutase (SOD) and methemoglobin (MetHb) were obtained from Sigma (St. Louis, USA). MTT, 3-(4,5-dimethyl-2-thiazolyl)-2,5-diphenyl-2H-tetrazolium bromide, and DTPA, diethylenetriamine-*N*,*N*,*N*′,*N*″,*N*″-pentaacetic acid, were purchased from Dojindo Laboratories (Kumamoto, Japan). *tert*-Butyl hydroperoxide (BHP) was from Katayama Chemical Industries (Osaka, Japan). 5,5-Dimethyl-1-pyrroline-1-oxide (DMPO) was obtained from Labotec (Tokyo, Japan). Black cloth made of a synthetic fiber was obtained from Nomura Tailor (Kyoto, Japan). All other chemicals used were of high-quality analytical grade.

Culture of human skin equivalent model (HSEM) and UVB exposure. HSEM (EpiDerm™ Skin Model, EPI-200) was purchased from MatTek Corporation (product # EPI-200-HCF; Ashland, MA, USA) and exposed to 13.5–67.5 mJ/cm^2 UVB exposure after 24 h cultivation. This model consists of normal human-derived epidermal keratinocytes, which has grown on permeable cell culture inserts that have the potential to form multi-layered and highly differentiated keratinocytes. The EpiDerm™ 200 samples were removed from the 24-well plates containing agarose and then transferred to the six-well plates containing 0.9 mL culture medium for 24 h cultivation at 37 °C in 5% CO_2 before the following experiments. After cultured for 24 h, the EpiDerm™ samples in the six-well plates with a fresh culture medium were exposed to UVB light. UVB was exposed at various doses of 13.5–67.5 mJ/cm^2 using FL20S · E lamps (Toshiba Medical Supply, Tokyo, Japan) as a light source, in which the exposure was measured by an Optix SafeSun Sensor as the precision UV meter (Optix Tech, Washington, DC, USA). Next, 25 μL of 100-μM CLA solution dissolved in 50% ethanol/H_2O was topically applied on the surface of skin samples immediately after UVB exposure. Measurement of chemiluminescent (CL) light emissions induced by the reaction with generated ROS was started at 2 min, as described below.

Ultra-low-light chemiluminescent detecting system. A luminograph (NightOWL Molecular Light Imager LB 981, EG&G Berthold, Germany) was used as a high-performance low-light imaging system for the detection of luminescent emissions (400–800 nm) [24]. The NightOWL possesses a Peltier-air-cooled CCD camera for ultra-low-light imaging with high sensitivity and is designed for macro imaging such as that of tissues or whole organisms. Its analytical performance is sufficient to evaluate the quantitative detection of ultra-low-light CL as described previously [4,5,15]. The luminescent signals on the photocathode in the image intensifier were detected as photons. The system was controlled by a DOS/V personal computer (OS: Microsoft Windows 98) provided with software for quantitative image analysis (WinLight 32, EG&G Berthold, Germany). The system was installed in an air-conditioned room (24 °C and 50% relative humidity).

Measurement of chemiluminescence due to ROS in the EpiDerm™ samples. The EpiDerm™ samples in the six-well plates were fixed on a warm pad at 37 °C and placed in a light-tight box to prevent interference by external light. The light emitted from the sample was allowed to accumulate for 5 min, treated with cosmic suppression for 1 min, followed by integration for approximately 20 s on the target of the camera tube, and was continuously measured at every 7 min for 60–180 min. The other instrumental settings were as follows: pixel size, 2 × 2; no background subtraction; camera readout, slow. The light emission outputs were recorded on a memory device. Quantification was expressed as the measurement of light from a single area of the sample. The background levels of CL intensities calculated for the black cloth below the sample were subtracted from the observed levels of those in the sample. The results of light emission intensities were expressed as photon/s/pixel. The area under the curve (AUC) plotted for the chemiluminescent signal intensity change in the sample vs. the time after UVB exposure was calculated by trapezoidal integration from zero time to the last observed time in order to evaluate time-dependent ROS generation [5].

In terms of measuring the early phases for CL profiles due to ROS generated in the EpiDerm™ samples with or without UVB exposure after CLA application, the CL intensities at 27 mJ/cm^2 UVB exposure and without UVB were measured for each 1 min during 30 s intervals. The other instrumental settings were the same as described above.

Measurement of CLA reactivity with ROS in the chemical generation system by ESR spin-trapping method. It was already shown that CLA reacts with $^{\cdot}O_2^-$ or $^1O_2$, and the CL emission is specifically induced by the reaction [14]. We also indicated that the CLA-dependent CL emissions were derived from the CLA/$^{\cdot}O_2^-$ and CLA/$^1O_2$ systems, but not from the CLA/$^{\cdot}$OH and CLA/H_2O_2 systems [25]. In addition, we here examined to confirm the reactivity of CLA with other ROS such as alkoxyl (RO$^{\cdot}$) and peroxyl (ROO$^{\cdot}$) radicals, as measured by ESR spin-trapping. Then, *tert*-butyl alkoxyl and peroxyl radicals were generated by the method of Akaike et al. [26], and the scavenging activity of CLA against these ROS was determined.

Twenty five millimolar BHP was added to 250 μg/mL MetHb in 100 mM phosphate buffer (pH 7.4) containing 25 μM DTPA and 10–100 μM CLA. Almost simultaneously, 50 mM DMPO was added to the solution. After mixing the solution on a vortex mixer for 30 s, ESR spectra due to DMPO-OOR and DMPO-OR were recorded on a JEOL FR-30 free radical monitor (Tokyo, Japan) at a field modulation frequency of 100 kHz, modulation amplitude of 0.1 mT, and an output power of 5 mW. Mn(II)O doped in MgO was used as a standard. After recording the ESR spectra, each signal intensity was normalized as a

relative signal height against the standard signal due to the Mn(II) marker. Reaction of CLA with both RO· and ROO· radicals was expressed as the scavenging activity against the ESR spectra due to their spin-adducts.

Identification of ROS generated in the EpiDerm™ samples with or without UVB exposure. Identification of ROS generated in the EpiDerm™ sample and the ability of topical applications with ROS scavengers such as SOD (100 μM in H_2O) and β-carotene (10 mM in 50% ethanol/PBS) were examined, in which each 10 μL of ROS scavengers and vehicle was applied for 10 min on the surface of treated and untreated EpiDerm™ samples before UVB exposure at a dose of 27 mJ/cm^2, respectively. No effects of each vehicle on the measurements were confirmed in advance. In addition, the washed effects of ROS scavengers were also examined in terms of removing the coating effect of scavengers as a UVB filter. Thus, all ROS scavengers were applied for 10 min on the surface of skin samples and then the skin samples were rinsed twice with 100 μL PBS before UVB exposure.

MTT assay for evaluation of cell survival after UVB exposure. MTT assay in terms of dehydrogenase activity in mitochondria was used for evaluation of cell survival ratio after 13.5–67.5 mJ/cm^2 UVB exposure [27]. The EpiDerm™ samples were transferred to the six-well plates containing 0.9 mL culture medium for 24 h cultivation at 37 °C in 5% CO_2. After cultured for 24 h, the EpiDerm™ samples in the six-well plates with a fresh culture medium were exposed to 13.5–67.5 mJ/cm^2 UVB light. Next, the samples were transferred to the 24-well plates containing 0.3 mL MTT solution (1 mg/ml) after UVB treatment and then continued to culture at 37 °C in 5% CO_2 incubator for 3 h. After 3 h incubation period with MTT, the samples were transferred to the pre-loaded 24-well extraction plates with each 2 mL of extractant (isopropyl alcohol:4 M HCl = 99:1, v/v), and the red-purple formazan produced by reduction of MTT was extracted under gentle swinging for 2 h. The absorbance due to formazan was determined at 570 nm using extractant as a blank. Background level for all samples at 650 nm was subtracted from the absorbance at 570 nm. The cell survival ratio was calculated from each absorbance of the formazan divided by that in negative control without UVB.

Statistical analysis. All experimental results are presented as the arithmetic mean values ± standard deviations (SDs) for 5–10 samples. The statistical analysis was performed using analysis of variance (ANOVA) followed by a post hoc test of Dunn's multiple comparison test at 5% ($P < 0.05$) or 1% ($P < 0.01$) significance levels.

Results and discussion

A typical visualization of time-dependent UVB-induced and intrinsic CL due to ROS produced in the EpiDerm™ samples is shown in Fig. 1. The 27 mJ/cm^2 UVB-exposed skin samples exhibited significantly higher CL levels (red color) than did the intact skin samples (green-yellow color), indicating the increased generation of ROS in the skin model. The quantified CL intensities due to UVB-induced ROS generation in the EpiDerm™ samples in terms of the areas under the curve of CL intensities (AUCs) exhibited the clearly higher levels in comparison with those due to intrinsic ROS generation in the intact cells (Table 1).

The significant difference in the intensity between intrinsic and UVB-induced CL in the EpiDerm™ samples suggested a difference in the chemical species of ROS in the cells. The chemical forms of ROS were then examined by topical application of a typical ROS scavenger and quencher. The application of SOD ($\cdot O_2^-$ scavenger) and BCR ($^1O_2$ quencher) greatly reduced UVB-induced CL intensities in the skin samples (Fig. 1). The UVB-exposed AUCs in the group treated with ROS scavenger or quencher were also significantly decreased in comparison with those without scavenger or quencher (Table 1). SOD slightly reduced intrinsic CL in the skin sample, whereas BCR barely did so (Fig. 1 and Table 1).

In addition, the washed effects of SOD and BCR were examined in the EpiDerm™ samples with or without UVB exposure. The reagents were topically applied for 10 min and then washed out by PBS in order to remove the coating effect due to remaining contents, which may act as a UVB filter. A scavenger and quencher greatly reduced UVB-induced CL intensities due to ROS generation and UVB-induced AUC values even after washing the reagents (Table 2), whereas no scavenger and quencher suppressed the intrinsic CL levels, and intrinsic AUC values were almost same as the control without treatment (Table 2). These data indicated that the remaining intrinsic CL seemed to be due to nonspecific luminescence other than ROS production in the intact EpiDerm™ sample.

SOD has been known to have dual abilities to scavenge $\cdot O_2^-$ (second-order rate constant $= 2.0 \times 10^9\ M^{-1}\ s^{-1}$) and quench $^1O_2$ (quenching rate constant $= 2.6 \times 10^9\ M^{-1}\ s^{-1}$) [28] and BCR typically quenches $^1O_2$ at the rate constant $= 3\text{–}30 \times 10^9\ M^{-1}\ s^{-1}$ [29]. BCR is also reported to scavenge alkyl (R·), alkoxyl (RO·), and peroxyl (ROO·) radicals [30], where the reaction of BCR with peroxyl radical (second-order rate constant $< 1.0 \times 10^6\ M^{-1}\ s^{-1}$) is indicated to be slower than with alkyl and alkoxyl radicals. In the present study, we demonstrated by ESR spin-trapping method that CLA does not almost react with both alkoxyl and peroxyl radicals, in which ESR spectra due to DMPO-OR and DMPO-OOR derived from BHP were not scavenged by adding 10–100 μM CLA to the solution (data not shown). In addition, CLA is reported not to react with alkyl radical including no oxygen atom [14]. Therefore, the CLA-dependent CL emission is concluded to be due to the reaction with $\cdot O_2^-$ and/or $^1O_2$. Consequently, it was indicated that the intrinsic CL was mostly due to nonspecific luminescence different from ROS, and that the UVB-induced CL was predominantly due to $\cdot O_2^-$ and $^1O_2$ in the EpiDerm™ sample. Measurement of the CL intensity during early period after 27 mJ/cm^2 UVB exposure exhibited already the significant difference between the intrinsic and UVB-induced CL levels (Fig. 2), supporting that the UVB-induced CL is due to the specific reaction of CLA with $\cdot O_2^-$ and $^1O_2$ generated in the upper layer of EpiDerm™ sample. We have previously demonstrated that $\cdot O_2^-$ is formed intrinsically and that both $^1O_2$ and $\cdot O_2^-$ are generated in the UVA-exposed skin of hairless mice at a dose of 18 J/cm^2 [15]. Recently, we found that the generation of $^1O_2$ and $\cdot O_2^-$ is induced in the skin of hairless mice even after UVB exposure over a dose of 100 mJ/cm^2 (data not shown). Although the sensitivity of response to UVB exposure might be different between the HSEM and hairless mice, it is useful to compare experimental results between two systems, and to evaluate protective ability of anti-oxidative agents in the HSEM system.

It is recently demonstrated in human keratinocytes that ROS such as $^1O_2$ and $\cdot O_2^-$ are generated in the UVB

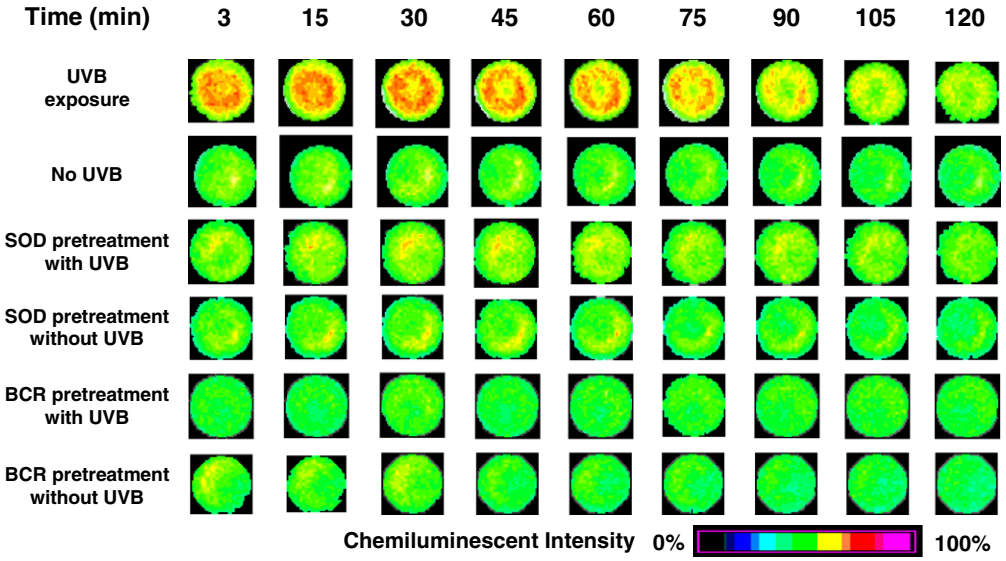

Fig. 1. Visualization of time-dependent ROS generation in the EpiDerm™ samples with or without UVB exposure, and scavenging effects of pretreatment with topically applied SOD and BCR before UVB exposure. Typical visualization and detection of the chemiluminescence due to ROS generation using CLA as the chemiluminescent probe were shown in the EpiDerm™ skin model for 120 min. The highest levels (red color) of ROS generation in the EpiDerm™ sample were found 15–30 min after UVB exposure at a dose of 27 mJ/cm^2. The low chemiluminescence (green-yellow color) was also observed in the skin model without UVB exposure. Ten microliter of SOD (100 μM in H_2O) or BCR (10 mM in 50% ethanol/PBS) was topically applied on the surface of EpiDerm™ samples before UVB exposure, exhibiting the remarkable scavenging effect on the UVB-induced ROS generation in the skin model.

Table 1
Suppressive effects of SOD and β-carotene on intrinsic and UVB-induced ROS generation in the EpiDerm™ skin model

	AUC (megaphotons/pixel)	
	Intrinsic	UVB exposed
Control	$18.6 \pm 2.2^{*}$	27.0 ± 3.9
SOD	15.6 ± 3.1	$19.1 \pm 2.7^{*,\#}$
β-Carotene	17.5 ± 2.5	$22.1 \pm 1.3^{*}$

Each 10 μL of SOD (100 μM) or β-carotene (10 mM) was topically applied to the EpiDerm™ skin model for 10 min before UVB exposure. AUC was measured for 0–115 min after the application of CLA. The data are expressed as means ± standard deviations for 8–10 samples in each experiment. Significance: $^{*}P < 0.01$ vs. control group with UVB exposure and $^{\#}P < 0.05$ vs. β-carotene-treated group with UVB-exposure.

Table 2
Washed effects of SOD and β-carotene on intrinsic and UVB-induced ROS generation in the EpiDerm™ skin model

	AUC (megaphotons/pixel)	
	Intrinsic	UVB exposed
Control	$4.6 \pm 0.6^{*}$	10.0 ± 1.9
SOD	4.9 ± 1.0	$3.9 \pm 0.9^{*,\#}$
β-Carotene	5.5 ± 1.1	$5.6 \pm 1.1^{*}$

Each 10 μL of SOD (100 μM) or β-carotene (10 mM) was topically applied to the EpiDerm™ skin model for 10 min and then washed twice by 100 μL PBS before UVB exposure. Then CLA was applied. AUC was measured for 0–52 min after the application of CLA. The data are expressed as means ± standard deviations for six samples in each experiment. Significance: $^{*}P < 0.01$ vs. control group with UVB exposure, and $^{\#}P < 0.05$ vs. β-carotene-treated group with UVB exposure.

light-stimulated photosensitization reaction of catalase [31], and that the electron-transport chain in mitochondrial such as Complex I and Complex III produces ROS such as

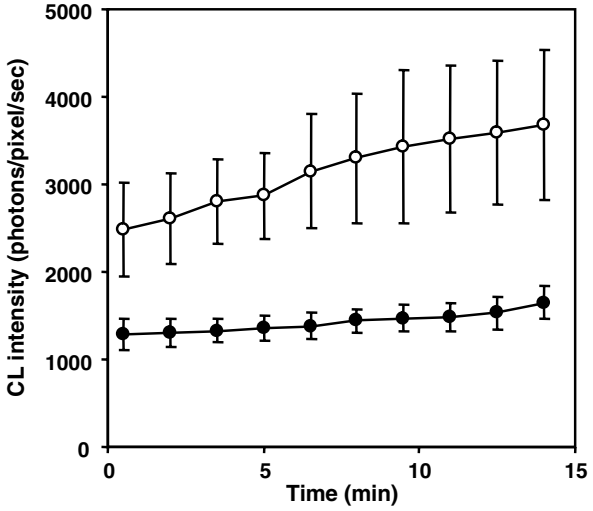

Fig. 2. Time-dependent profiles of the quantified chemiluminescent intensity due to ROS generated in the EpiDerm™ samples with or without UVB exposure during early periods after CLA application. The CL intensities after UVB exposure at 27 mJ/cm^2 (○) and those without UVB (●) were measured for 1 min during 30 s intervals. The significant difference ($P < 0.01$) in CL intensities between the intrinsic and UVB-exposed skin samples was found for all measured time after UVB exposure and CLA application.

$^1O_2$ and $\cdot O_2^-$ [32,33]. In addition, several studies indicated that $^1O_2$ and $\cdot O_2^-$ generation after UVB excitation in the keratinocytes of skin results in UVB-induced damage of the skin [34]. We demonstrated here evidence for the UVB-induced formation of $^1O_2$ and $\cdot O_2^-$ in the human keratynocyte skin model.

Because $^1O_2$ and $\cdot O_2^-$ were triggered to produce in the skin model at a dose of 27 mJ/cm^2 UVB, we then examined the relationship between the UVB dose and CL intensity due to induced ROS generation. Although the EpiDerm™ samples were exposed under UVB light at the several doses of 13.5–67.5 mJ/cm^2, the UVB dose–response of mean CL intensities was only observed at the range of 13.5–27 mJ/cm^2 as shown in Fig. 3. Whereas, mean CL intensities at 40.5 mJ/cm^2 were almost same as for the intrinsic levels, and those at 67.5 mJ/cm^2 were significantly decreased in comparison with the intrinsic levels. These results suggested that the skin models are inactivated or toxicated by a higher dose of UVB exposure over 27 mJ/cm^2. The UVB dose-dependent cell viability was also evaluated by MTT assay. When the EpiDerm™ samples were exposed to UVB light at 13.5–67.5 mJ/cm^2, the formazan, which was produced through the reduction of MTT by dehydrogenase in mitochondria, was significantly decreased in a UVB dose-dependent manner (Fig. 4), indicating that UVB exposure over 27 mJ/cm^2 exhibited cytotoxic effects on the skin samples through the mitochondria damage. Thus, the CL intensity due to UVB-induced ROS generation, which seems to partly produce form the electron-transport chain in mitochondria, may be reduced in the EpiDerm™ sample after UVB exposure at the higher doses.

The time- and space-dependent dynamics of ROS generation from the cultured human models with non-invasive condition have not been previously reported except for one report [23]. The real-time monitoring of cell-dependent CL changes due to $\cdot O_2^-$ and/or $^1O_2$ is achieved in the present study, by means of a sensitive two-dimensional ultra-low light luminograph, NightOwl. We have already reported in animal's study that the method constitutes a strong tool for investigating the skin response to UV light stress, especially in regard to the detection of oxidative stress processes and the evaluation of antioxidants for the skin [4,5,15]. The new technique proposed here will determine the features of endogenously generated ROS in the HSEM and provide the simple, convenient, and convincing evaluation for protective effects of antioxidant and photoprotective agents on UV-induced oxidative stress in the HSEM.

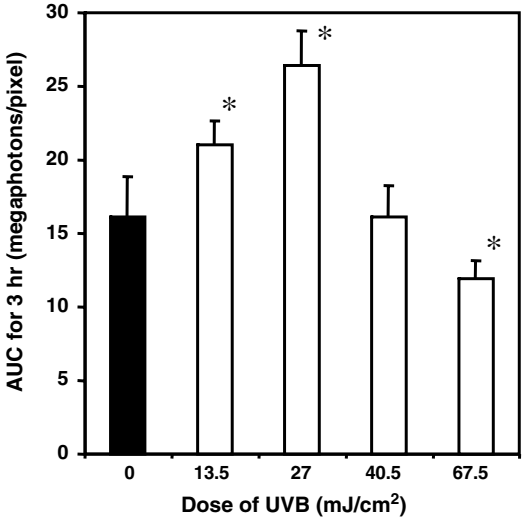

Fig. 3. UVB dose-dependency on the chemiluminescent intensities due to ROS generation in the EpiDerm™ samples. The EpiDerm™ samples were exposed to UVB light at various doses of 13.5–67.5 mJ/cm^2. The AUC for the chemiluminescent signal intensity profile vs. the time after UVB exposure was calculated by trapezoidal integration from zero time to the last observed time. The data are expressed as means ± standard deviations (numbers of cells = 5–7 in each dose). Significance: $*P < 0.01$ vs. control group without UVB exposure.

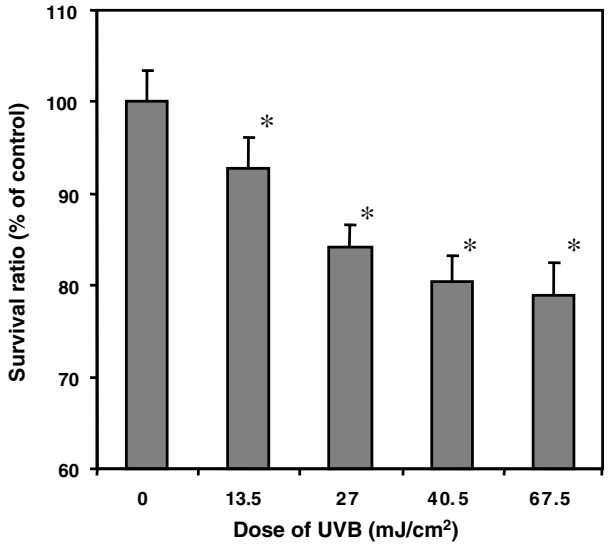

Fig. 4. UVB dose-dependency on the cell viability as evaluated by MTT assay. The EpiDerm™ samples were exposed to UVB light at 13.5–67.5 mJ/cm^2. The formazan produced through the reduction of MTT by dehydrogenase in mitochondria was extracted and its absorbance was determined at 570 nm. The data are expressed as means ± standard deviations (numbers of cell = 8 in each dose). Significance: $*P < 0.01$ vs. control group without UVB exposure.

In conclusion, the weak CL due to non-specific luminescence was observed in the intact EpiDerm™ group without UVB treatment. Whereas, in the UVB-treated EpiDerm™ group, the CL intensity due to endogenous ROS generation increased significantly in comparison with that in the intact group, its maximum being observed at a dose of 27 mJ/cm^2. ROS under UVB exposure was identified to be $^1O_2$ and $\cdot O_2^-$ by suppressive effects of ROS scavengers topically applied on the skin model. The results for UVB-induced ROS generation in the HSEM were consistent with those observed in the skin of live animals. EpiDerm™ 200 as three-dimensional HSEM was shown to be useful system not only to predict UVB-induced ROS-related skin responses in human but also to find the protective agents against UVB-induced oxidative stress in place of animals and *ex vivo* human skin.

Acknowledgment

This study was supported by The Procter & Gamble Company.

References

[1] M. Ichihashi, M. Ueda, A. Budiyanto, T. Bito, M. Oka, M. Fukunaga, K. Tsuru, T. Horikawa, UV-induced skin damage, Toxicology 189 (2003) 21–39.

[2] M.L. Kripke, P.A. Cox, L.G. Alas, D.B. Yarosh, Pyrimidine dimmers in DNA initiate systemic immunosuppression in UV-irradiated mice, Proc. Natl. Acad. Sci. USA 89 (1992) 7516–7520.

[3] N. Bech-Thomsen, H.C. Wulf, Carcinogenic and melanogenic effects of a filtered metal halide UVA source and a tubular fluorescent UVA tanning source with or without additional solar-simulated UV radiation in hairless mice, Photochem. Photobiol. 62 (1995) 773–779.

[4] H. Yasui, H. Sakurai, Chemiluminescent detection and imaging of reactive oxygen species in live mouse skin exposed to UVA, Biochem. Biophys. Res. Commun. 269 (2000) 131–136.

[5] H. Yasui, H. Sakurai, Age-dependent generation of reactive oxygen species in the skin of live hairless rats exposed to UVA light, Exp. Dermatol. 12 (2003) 655–661.

[6] E.H. Lee, D. Faulhaber, K.M. Hanson, W. Ding, S. Peters, S. Kodali, R.D. Granstein, Dietary lutein reduces ultraviolet radiation-induced inflammation and immunosuppression, J. Invest. Dermatol. 122 (2004) 510–517.

[7] P. Larsson, E. Andersson, U. Johansson, K. Öllinger, I. Rosdahl, Ultraviolet A and B affect human melanocytes and keratinocytes differently. A study of oxidative alterations and apoptosis, Exp. Dermatol. 14 (2005) 117–123.

[8] H. Sasaki, H. Akamatsu, T. Horio, Protective role of copper, zinc superoxide dismutase against UVB-induced injury of the human keratinocyte cell line HaCaT, J. Invest. Dermatol. 114 (2000) 502–507.

[9] L. Hellemans, H. Corstjens, A. Neven, L. Declercq, D. Maes, Antioxidant enzyme activity in human stratum corneum shows seasonal variation with an age-dependent recovery, J. Invest. Dermatol. 120 (2003) 434–439.

[10] H. Ou-Yang, G. Stamatas, C. Saliou, N. Kollias, A chemiluminescence study of UVA-induced oxidative stress in human skin in vivo, J. Invest. Dermatol. 122 (2004) 1020–1029.

[11] G. Sauermann, W.P. Mei, U. Hoppe, F. Stäb, Ultraweak photon emission of human skin in vivo: influence of topically applied antioxidants on human skin, Methods Enzymol. 300 (1999) 419–428.

[12] K.M. Hanson, R.M. Clegg, Observation and quantification of ultraviolet-induced reactive oxygen species in ex vivo human skin, Photochem. Photobiol. 76 (2002) 57–63.

[13] G. He, V.K. Kutala, P. Kuppusamy, J.L. Zweier, In vivo measurement and mapping of skin redox stress induced by ultraviolet light exposure, Free Rad. Biol. Med. 36 (2004) 665–672.

[14] M. Nakano, Determination of superoxide radical and singlet oxygen based on chemiluminescence of luciferin analogs, Methods Enzymol. 186 (1990) 585–591.

[15] H. Sakurai, H. Yasui, Y. Yamada, H. Nishimura, M. Shigemoto, Detection of reactive oxygen species in the skin of live mice and rats exposed to UVA light: a research review on chemiluminescence and trials for UVA protection, Photochem. Photobiol. Sci. 4 (2005) 715–720.

[16] E. Bell, H.P. Ehrlich, D.J. Buttle, T. Nakatsuji, Living tissue formed in vitro and accepted as skin-equivalent tissue of full thickness, Science 211 (1981) 1052–1054.

[17] F. Bernerd, D. Asselineau, Successive alteration and recovery of epidermal differentiation and morphogenesis after specific UVB-damages in skin reconstructed in vitro, Dev. Biol. 183 (1997) 123–138.

[18] F. Bernerd, C. Vioux, D. Asselineau, Evaluation of the protective effect of sunscreens on in vitro reconstructed human skin exposed to UVB or UVA irradiation, Photochem. Photobiol. 71 (2000) 314–320.

[19] C. Duval, R. Schmidt, M. Regnier, V. Facy, D. Asselineau, F. Bernerd, The use of reconstructed human skin to evaluate UV-induced modifications and sunscreen efficacy, Exp. Dermatol. 12 (suppl. 2) (2003) 64–70.

[20] M.A. Perkins, R. Osborne, F.R. Rana, A. Ghassemi, M.K. Robinson, Comparison of in vitro and in vivo human skin responses to consumer products and ingredients with a range of irritancy potential, Toxicol. Sci. 48 (1999) 218–229.

[21] M. Ponec, E. Boelsma, S. Gibbs, M. Mommaas, Characterization of reconstructed skin models, Skin Pharmacol. Appl. Skin Physiol. 15 (suppl. 1) (2002) 4–17.

[22] C. Faller, M. Bracher, Reconstructed skin kits: reproducibility of cutaneous irritancy testing, Skin Pharmacol. Appl. Skin Physiol. 15 (suppl. 1) (2002) 74–91.

[23] K.M. Hanson, R.M. Clegg, Two-photon fluorescence imaging and reactive oxygen species detection within the epidermis, Methods Mol. Biol. 289 (2004) 413–421.

[24] A. Roda, P. Pasini, M. Musiani, S. Girotti, M. Baraldini, G. Garrea, A. Suozzi, Chemiluminescent low-light imaging of biospecific reactions on macro- and microsamples using a videocamera-based luminograph, Anal. Chem. 68 (1996) 1073–1080.

[25] R. Tawa, H. Sakurai, Determination of four active oxygen species such as H_2O_2, $^{\cdot}OH$, $^{\cdot}O_2^-$, and $^1O_2$ by luminol- and CLA-chemiluminescence methods and evaluation of antioxidative effects of hydroxybenzoic acids, Anal. Lett. 30 (1997) 2811–2825.

[26] T. Akaike, K. Sato, S. Ijiri, Y. Miyamoto, M. Kohno, M. Ando, H. Maeda, Bactericidal activity of alkyl peroxyl radicals generated by heme–iron-catalyzed decomposition of organic peroxides, Arch. Biochem. Biophys. 294 (1992) 55–63.

[27] T. Mosmann, Rapid colorimetric assay for cellular growth and survival, application to proliferation and cytotoxicity assay, J. Immunol. Methods 65 (1983) 55–63.

[28] G. Rotilio, R.C. Bray, E.M. Fielden, A pulse radiolysis study of superoxide dismutase, Biochim. Biophys. Acta 268 (1972) 605–609.

[29] A. Cantrell, D.J. McGarvey, T.G. Truscott, F. Rancan, F. Böhm, Singlet oxygen quenching by dietary carotenoids in a model membrane environment, Arch. Biochem. Biophys. 412 (2003) 47–54.

[30] A. Mortensen, L.H. Skibsted, Reactivity of β-carotene towards peroxyl radicals studied by laser flash and steady-state photolysis, FEBS Lett. 426 (1998) 392–396.

[31] D.E. Heck, A.M. Vetrano, T.M. Mariano, J.D. Laskin, UVB light stimulates production of reactive oxygen species: unexpected role for catalase, J. Biol. Chem. 278 (2003) 22432–22436.

[32] M. Berneburg, S. Grether-Beck, V. Kürten, T. Ruzicka, K. Briviba, H. Sies, J. Krutmann, Singlet oxygen mediates the UVA-induced generation of the photoaging-associated mitochondrial common deletion, J. Biol. Chem. 274 (1999) 15345–15349.

[33] Q. Chen, E.J. Vazquez, S. Moghaddas, C.L. Hoppel, E.J. Lesnefsky, Production of reactive oxygen species by mitochondria: central role of complex III, J. Biol. Chem. 278 (2003) 36027–36031.

[34] B.A. Jurkiewicz, G.R. Buettner, EPR detection of free radicals in UV-irradiated skin: mouse versus human, Photochem. Photobiol. 64 (1996) 918–922.